Laboratory Investigation of an Ultra-Low NO$_x$ Premixed Combustion Concept for Industrial Boilers

David Littlejohn, Adrian J. Majeski, Shaheen Tonse, Carlo Castaldini[*] and Robert K. Cheng
Lawrence Berkeley National Laboratory
Berkeley, California, 94720 USA

[*] CMC Engineering
1455 Bittern Drive
Sunnyvale, CA 94087 USA

Corresponding author: David Littlejohn
Lawrence Berkeley National Laboratory
MS 70-108B, 1 Cyclotron Road
Berkeley, CA 94720
USA

Voice: 510 486 7598
Fax: 510 486 7303
E-mail: Dlittlejohn@lbl.gov

Word Count	
Lines of text 15 x 214	3210
Equations 9 x 21	189
Figures 9 x 200	1800
References 7 x 31	217
Total	5416

Colloquium: New Concepts in Combustion Technology

Keywords: lean premixed burners, industrial boilers, fuel reforming, catalyst, emission control

Laboratory Investigation of an Ultra-Low NO$_x$ Premixed Combustion Concept for Industrial Boilers

David Littlejohn, Adrian J. Majeski, Shaheen Tonse, Carlo Castaldini[*] and Robert K. Cheng

Lawrence Berkeley National Laboratory
Berkeley, California 94720 USA

[*]CMC Engineering
1455 Bittern Drive
Sunnyvale, California 94087 USA

Abstract

A combustion concept to achieve ultra-low emissions (NO$_x \le 2$ ppm and CO ≤ 20 ppm) was tested on an 18 kW low swirl burner (LSB). It is based on lean premixed combustion combined with flue gas recirculation (FGR) and partially reformed natural gas (PRNG). Flame stability and emissions were assessed as a function of ϕ, FGR, and PRNG. The results show that PRNG improves flame stability and reduces CO, with no impact on NO$_x$ at $\phi = 0.8$. A 1D flame simulation satisfactorily predicted prompt NO$_x$ at lean conditions with high FGR. Two catalysts were tested in a prototype steam reformer, and the results were used to estimate reactor volume and steam requirements in a practical system. An advanced Sud Chemie catalyst displayed good conversion efficiency at relatively low temperatures and high space velocities, which indicates that the reformer can be small and will track load changes. Tests conducted on the LSB with FGR and 0.05 PRNG shows that boilers using a LSB with PRNG and high FGR and ϕ close to stoichiometry can operate with low emissions and high efficiency.

Introduction

In recent years, lean premixed combustion has gained eminence as an effective control technology to reduce NO_x from industrial natural gas (NG) systems [1-3]. This progress owes largely to burner designs that harness the dynamic nature of lean premixed flames and their instability tendencies towards the lean limit [4]. However, most premixed burners are complex, tightly controlled, and expensive for small to mid-sized industrial applications. As many US regions are adopting more stringent environmental regulations, equipment manufacturers require reliable, low-cost solutions that can meet $NO_x < 9$ ppm limit (corrected to 3% O_2). To achieve the 2 ppm NO_x goal proposed by the Office of Industrial Technology of the US Department of Energy for year 2020, a new approach is required because NG flames that can reach this target are almost at the theoretical flammability limit.

Our objective is to study a promising methodology that may enable industrial systems to access the < 2 ppm NO_x goal without sacrificing CO emissions or system efficiency. The approach is to merge an advanced premixed burner with gas pretreatment. Our low-swirl burner (LSB) [5, 6] is simple and robust. It is being commercialized for industrial applications of up to 3 MW. To access 2 ppm NO_x, the strategy is to use FGR and optimize the LSB for burning partially reformed natural gas (PRNG). Reforming part of the NG to H_2 and CO_2 can provide the critical stability margin at the ultra lean conditions as well as lower CO levels [7].

This paper reports the results of a study of this concept for steam boilers (Figure 1). The convective section offers a convenient location for a catalytic reformer where steam and high temperature are available. To meet size restriction*s*, load flexibility, and emission targets, the reformer reforms a portion of the fuel stream. Because external FGR is relatively common in most low-emission boilers, the existing flow supplies and fuel/air mixer can be used for the burner. Practical implementation of this concept will require knowledge on (1) the effects of equivalence ratio, ϕ, FGR*,* and PRNG on LSB operability, (2) the required NG/FGR/PRNG ratio and ϕ to achieve $NO_x \leq 2$ ppm and CO ≤ 20 ppm, and (3) conversion efficiency of steam reforming to estimate the reformer size. Laboratory experiments were performed to determine the LSB emissions using simulated FGR/PRNG. The conversion efficienc*y* of steam reforming at boiler conditions was also investigated. The concept of Figure 1 was verified in a water heater simulator [6] that incorporated a reformer and external FGR. The data were compared with theoretical calculations obtained for 1D laminar flame. Our results are very encouraging and show that this concept offer*s* an effective option for industrial systems.

Experimental Setups and Flame Calculation

Low-swirl burner

The LSB was developed in 1991 [8]. Laboratory studies [8-10] showed that the LSB generates divergent flows to allow free propagation of turbulent premixed flames. In LSBs, the displacement flame speeds, S_T, at leading edge of the flame brush scale linearly with rms velocity, u'. This is quite different than S_T reported that tend to level off at high u' [10]. For practical applications, a patented vane-swirler has been developed [11]. It is different than conventional swirlers [12-14] and features a centerbody that allows a portion of the reactants to bypass the swirl annulus [5]. Centerbody screens with different blockages control the ratio of the flows through the centerbody and the swirl vanes. The definition of the swirl number for the LSB may require an estimation of the flow velocities [5]. Equation (1) is a more practical form expressed in terms of $R = R_c/R_b$ the ratio of the radii of the burner, R_b, and the centerbody, R_c, the vane angle, α, and $m = \dot{m}_c / \dot{m}_a$ the ratio of mass fluxes (flow-split) through the centerbody ($\dot{m}_c$) and annulus ($\dot{m}_a$). The value m can be determined by measuring separately the pressure drops across the centerbody and the vane annulus using standard procedures in gas turbine development [15].

$$S = \frac{2}{3}\tan\alpha \frac{1 - R^3}{1 - R^2 + [m^2 (1/R^2 - 1)^2]R^2} \quad (1)$$

The swirl number, S, and the swirler recess distance, L, determine the LSB operating regime. To optimize for FGR and PRNG, we used a LSB with $R_b = 2.6$ cm, $R_c = 2.0$ cm ($R = 0.776$) and eight straight vanes at $\alpha = 37°$[16]. A 71% screen (a perforated plate) was used in this study. The minimum m necessary for stable operation is about 1 and S is in the order of 0.4 [15]. This LSB is robust and can operate up to 600 kW. It enables us to investigate the effects of FGR and PRNG and gain knowledge applicable to industrial systems. The LSB was chosen to test our concept because it has a wide range of stable operating conditions.

Flame model

One of the most challenging tasks in industrial system development is the prediction of the pollutant formation. Industrial burners have complex flame properties due to high shear, turbulent mixing (of fuel, air and flue gas) and staging. Consequently, proper choice of the flame models (premixed, non-premixed, or partially premixed) for different regions of the large flame can be critical to the fidelity of the simulations. In contrast, flames in LSBs are

not subject to these complexities. Measurements [10, 17] show that they exhibit wrinkled flamelet structures even under intense turbulence. This implies that a premixed flame model may be sufficient for LSB flames. If this approach proves tractable, it can greatly simplify the requirements of the numerical tools for developing LSBs for industrial applications.

The current experiments (at 18 kW) provide a logical starting point to evaluate the appropriateness of using a simple flame model. At conditions close to the lowest operating velocities and turbulence levels, the flame is lifted. Upstream heat transfer is negligible and the transverse stretch rate is very low [9], allowing use of a 1D laminar premixed flame approximation. We used the Chemkin application Premix [18] to find steady-state solutions for compositions corresponding to those generated by the reformer with real FGR. GRI-Mech 3.0 with 53 species for CH_4 combustion containing both prompt and thermal NO_x reactions was employed [19]. Within Premix, the Chemkin (version 2.5) library [20] was used for thermodynamic and kinetic calculations. To be consistent with the water heater measurements (see below), a calculation time equivalent to the system residence time (100 ms) was used. This criterion was estimated from the velocity at the trailing edge of the flame brush (1 m/s) [6] and the distance to the heat exchanger (10 cm).

Water heater simulator

An 18 kW water heater simulator [6] was used to evaluate the LSB as a function of ϕ, FGR, and PRNG (Figure 2). It employs a chamber/heat-exchanger assembly (20 x 16.5 x 23 cm). The LSB is sealed 18 cm below the heat exchanger. The flue radius is 5 cm with a 50 cm duct. The fuel mixture is introduced at 1 m upstream of the burner to ensure thorough mixing. All the experiments were performed at 18 kW with 15 l/m of water into the heat exchanger. The exhaust is sampled at 4 cm below the duct exit with a stainless steel tube. The exhaust flows through a water trap and desiccant and into NO_x, CO, and O_2 analyzers.

The first set of experiments used simulated FGR and PRNG to obtain a reference data set that is not influenced by steam and flue gas variations. ϕ for this system is defined by:

$$\phi = (2* \dot{v}_{CH_4} + 0.5 * \dot{v}_{H_2}) / (0.209 * \dot{v}_{Air}) \qquad (2)$$

Using the volumetric flow rate of air, $\dot{v}_{Air}$, and set values of ϕ, FGR and PRNG, the PC controls the flow rates for $\dot{v}_{CH_4}$, $\dot{v}_{H_2}$ $\dot{v}_{N_2}$, $\dot{v}_{CO_2}$ according to:

$$\dot{v}_{CH_4} = \dot{v}_{Air} * \phi * 0.209 / (2 + 0.5 * PRNG * 0.8) \qquad (3)$$

$$\dot{v}_{CO_2} = \dot{v}_{Air} * FGR * 0.12 + \dot{v}_{CH_4} * PRNG * 0.2 \qquad (4)$$
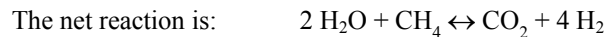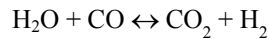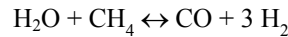
$$\dot{v}_{N_2} = \dot{v}_{Air} * FGR * 0.88 \qquad (5)$$

$$\dot{v}_{H_2} = \dot{v}_{CH_4} * PRNG * 0.8 \qquad (6)$$

The second set of experiments was a full simulation of the concept using real FGR and PRNG supplied by a steam reformer described below. Flue gases are pumped off, dried, and metered by a turbine meter before being mixed with the air and fuel mixture.

Steam reformer

Hydrogen is generated commercially with steam reformers where natural gas is mixed with steam and flowed over a nickel-based catalyst at 1000-1200 K. The mixture equilibrates with hydrogen and carbon dioxide according to:

$$H_2O + CH_4 \leftrightarrow CO + 3\ H_2$$

$$H_2O + CO \leftrightarrow CO_2 + H_2$$

The net reaction is: $\qquad 2\ H_2O + CH_4 \leftrightarrow CO_2 + 4\ H_2$

Excess steam helps drive the reaction to the right, increasing the proportion of hydrogen and carbon dioxide.

Limited data on partial reforming is available because the emphasis had been on maximum H_2 production. The goal of our experiment*s* is therefore to obtain data on conversion efficiency (percent of methane converted) as a function of steam input, temperature, and space velocity. Such knowledge is needed to determine the reformer volume and operating conditions for industrial systems and to estimate the impact on overall efficiency.

The laboratory reformer (Figure 1) uses 1.5 kW tube furnaces to generate steam (0.04 – 0.12 l/s) and to heat the catalyst. Metered CH_4 (0.01 – 0.04 l/s) was mixed with steam and fed into the catalyst in a 2.5 cm I.D. stainless steel

tube. Two different catalysts were evaluated: a standard reformer catalyst (NiO on alumina) and an advanced Sud Chemie catalyst (on a Corning cellular cordierite support). The inlet of the reformer was < 120 kPa and its temperature (500 – 800 C) was controlled to ± 2 C. After removing steam from the reformer output, the concentrations of CH_4, CO_2, and CO were measured by infrared spectroscopy (Nicolet 760 FTIR) and the H_2 concentration was measured by gas chromatography (SRI 8610).

Results

Operability of LSBs with FGR and PRNG

At 18 kW, the LSB operates at a reference velocity (the flow averaged over the burner cross-section) of $U_o \approx 3$ m/s. Velocity measurements have shown that its flowfields has yet to reach a self-similarity form and lean blow-off (LBO) is at its lowest [23]. This condition can be considered as optimum for flame stability with FGR and PRNG. Flame stability and LBO were determined for $0.7 < \phi < 0.9$, $0 < FGR < 0.3$ and $0 < PRNG < 0.3$. At $\phi = 0.8$ and 0.9, all flames remain stable. At $\phi = 0.7$ and PRNG = 0.0, a stable flame could not be sustained with FGR > 0.2. However, increasing PRNG to 0.1 allowed the flame to recover and the blow-off limit shifted to FGR = 0.25. With PRNG > 0.25, the LSB operates reliably with FGR up to 0.28. This result demonstrates the effectiveness of H_2 in PRNG to promote flame stability under high FGR dilution.

These results confirm the LSB design can be scaled to larger sizes. To evaluate the LSB concept up to 2 MW, two burners (R_b = 6.4 and 9.2 cm) were built. The R_b = 6.4 cm burner has different types of straight and curved vanes to minimize pressure drop. Both larger burners were tested in boiler simulators with real FGR and showed stable operation. The type of vane did affect LSB performance. At 0.6 MW and $\phi = 0.7$, the R_b = 6.4 cm LSB accepted FGR = 0.3. The fact that the larger LSB at $U_o \approx 20$ m/s tolerates a larger amount of FGR than a small burner at $U_o \approx 3$ m/s strongly suggest*s* that the self-similar features of the LSB are important for turndown. Since the data show*s* that the addition of PRNG improves LBO, the larger LSBs should also accept PRNG.

LSB emissions with simulated FGR/PRNG

NO_x and CO emissions (corrected to 3% O_2) of the water heater are shown in Figure 3. The effectiveness of FGR in reducing NO_x is apparent by the exponential decay of the three data sets. It is clear that PRNG has no significant effect on NO_x. At $\phi = 0.7$ where NO_x emissions are < 20 ppm, the scatter in the data for $0 < PRNG < 0.3$ are well

within experimental uncertainty. In contrast, CO emissions show more complex trends. At $\phi = 0.9$, CO remains at a high level of 50 to 80 ppm. Adding PRNG lowers CO to 30 ppm with FGR > 0.2. At $\phi = 0.8$, PRNG is more effective in lowering CO and a significant reduction is found for PRNG > 0.2. The CO emissions at $\phi = 0.7$ increase rapidly with FGR > 0.1. Introducing PRNG also lowers CO but cannot achieve the same effectiveness as found at $\phi = 0.8$. Thus PRNG improves flame stability and CO burnout, while FGR provides dilution that lowers thermal NO_x production.

These NO_x and CO data define the operating conditions that will meet various NO_x-CO criteria. To achieve $NO_x < 5$ ppm and CO < 20 ppm, a fairly wide regime at $\phi = 0.8$, $0.15 < FGR < 0.25$, and $0.1 < PRNG < 0.3$ is available. The regime grows substantially if the criteria are relaxed to $NO_x < 9$ ppm and CO < 40 ppm. However, the $NO_x < 2$ ppm and CO < 20 ppm condition is only within reach at $\phi = 0.8$, FGR = 0.3 and PRNG = 0.24. The main implication is that meeting stringent emission limits requires very tight burner control.

Flame simulation

Figure 4 shows the NO_x emissions obtained from 1D flame calculations and the adiabatic flame temperature $T_{ad} = 1800$ K contour. Though the calculated NO_x data exhibit the same exponential decay with FGR and an absence of PRNG dependence observed in the experiments, the calculated levels can be an order of magnitude higher, especially at $\phi = 0.9$ (compare with Figure 3). It is apparent that the calculations and experiments are more consistent for $T_{ad} < 1800$ K where thermal NO_x is suppressed. This includes all the $\phi = 0.7$ cases, and $\phi = 0.8$ and FGR > 0.2 cases and shows that lean flames produce primarily prompt NO_x. Recall that the calculations used a 100 ms criterion to simulate the residence time of the products in the heat exchanger. Therefore, the combustion products remain at T_{ad} and promote thermal NO_x. In the water heater, temperature of the products decay rapidly due to heat transfer and mixing with the surrounding gases and thus quench the formation of thermal NO_x. A better comparison with the experiments can be achieved by using a 10 ms criterion. The fact that NO_x predictions for the high FGR cases are unchanged when using the 10 ms criterion further supports the argument on thermal NO_x. This suggests that the treatment of the temperature and fluid fields downstream of the flame is important to predicting NO_x formation in a LSB system.

The prediction of CO emissions is not at all satisfactory. The results are at least an order of magnitude higher and have exponential decay trends that are the opposite of most of the measurements. Even for cases without FGR or

8

PRNG, the calculations do not show CO increasing with decreasing ϕ as observed experimentally. There are several factors that contribute to the failure in CO prediction. The 1D flame model generates CO levels that agree well with CO concentrations that are in equilibrium with the combustion products at T_{ad}. However, the equilibrium CO concentrations are substantially higher than those measured in the LSB exhaust. Practical flames increase the oxidation of CO in the exhaust by processes that are not present in the 1D model. As stated by Bowman [21], calculation of CO from practical combustion devices requires a coupling of the CO mechanism with a combustion chamber model. The choice of the semi-empirical models can be critical. As our goal is to explore the usefulness of a simple 1D flame model for LSB, we conclude that it can be quite precise in predicting prompt NO_x for the lean and highly dilute cases.

Partial reforming and proof of overall concept

The conversion efficiencies, ε_c, for the two catalysts as function of the gas hour space velocity, S_v, are compared in Figure 5. S_v is defined as the reformer volume divided by input flow rate at STP. The ε_c of the conventional NiO catalyst was found to drop rapidly with increasing S_v even at relatively high reforming temperatures of 700 to 800 C and fell to $\varepsilon_c = 0.3$ at S_v of only 6000. In contrast, the Sud Chemie advanced catalyst can match the ε_c of NiO at a lower temperature of 650 C. More importantly, ε_c at temperatures of 500 to 650 C shows a leveling trend with increasing S_v up to 30,000. The significance of this trend is that the reformer can be more compact and sufficiently flexible to handle load changes. Also, operating at lower temperatures reduces CO formation and improves system efficiency. These results show that the choice of catalyst will be significant for the implementation of our scheme for different boilers.

To confirm the feasibility of our concept, the reformer with the Sud Chemie catalyst and an external FGR circuit was integrated to the water heater. The experiments covered $0.7 < \phi < 0.9$, $0 < FGR < 0.3$ with or without PRNG = 0.05. The supply of PRNG required a 650 C reformer temperature and steam and CH_4 flow rates of 0.12 and 0.04 l/s respectively ($S_v = 10,000$). The results showed that the operating domain of the LSB with real FGR/PRNG was essentially the same as that found with simulated FGR/PRNG. Therefore, adding $\approx 5\%$ steam to the premixture does not affect LSB operation. The NO_x and CO emissions are shown in Figure 6. The real FGR/PRNG experiments also showed that PRNG has no effect on NO_x and are consistent with the simulated FGR/PRNG results. However, the use of real FGR/PRNG generated a higher level of NO_x. At $\phi = 0.9$ and FGR = 0.28, NO_x remains above 10 ppm.

9

The results at $\phi = 0.7$ and 0.8 also indicate that a larger amount of FGR would be needed to attain the 5 ppm threshold and none of the experiments was able to reach the $NO_x < 2$ ppm target. This seems to indicate that the control of NO_x at the so-called single-digit level of < 10 ppm is quite arduous.

The trends of the CO emissions in Figure 6 were generally consistent with those from simulated FGR/PRNG. At $\phi = 0.9$, CO decreased with increasing FGR and the introduction of PRNG = 0.05 had no observable effect. As in Figure 3, minimum CO levels were achieved at $\phi = 0.8$, but real FGR delivers an extended range of conditions (0.08 < FGR < 0.2) where CO remained at 10 ppm. The use of PRNG = 0.05 from the reformer had a more significant effect on CO reduction compared the simulated PRNG runs and the difference may be attributed to the presence of steam. The NO_x and CO data shows $NO_x < 5$ ppm and CO < 20 ppm is achieved in a narrow regime at $\phi = 0.8$, 0.2 < FGR < 0.24 and 0 < PRNG < 0.05. If $NO_x < 9$ ppm and CO < 40 ppm were used, the regime grows to 0.1 < FGR < 0.24.

The technological feasibility of our combined LSB/FGR/PRNG methodology is confirmed by these results. However, economical implementation in steam boilers needs optimization of the reformer volume and operating conditions. From results of Figure 5, the normalized reformer volume (liter/MW) for steam boilers is calculated (Figure 7). These calculations use a conservative 0.1 = PRNG rather than 0.05 = PRNG and can be generalized as they scale directly with thermal input and PRNG. Reformer volumes of 2 to 10 liter/MW are not unreasonable in a typical 1 MW boiler system that has a radiant section of approximately 2.5 m by 0.75 m. However, the Sud Chemie catalyst shows that at $S_v < 10000$, a 150 C decrease in reforming temperature can increase the reformer volume by a factor of 4. The most encouraging result is that the volume of the reformer for 600 to 650 C shows little dependence on S_v and is relatively flat at 2 to 3 liters/MW. This implies that the reformer can be small and can follow the load without changing the feed rate to the reformer. To accommodate the load range, the design point should be close to the maximum S_v. When the burner is turned down, the reformer should be able to produce the right amount of reform gas down to $S_v = 10,000$. If operated at $S_v < 10000$, the reformer will produce a higher amount of PRNG than needed. This advantageous because a higher level of H_2 will promote flame stability. This suggests that the reformer will function well in load following.

Conclusions

The overall LSB/FGR/PRNG concept to achieve NO_x levels approaching 2 ppm with low CO and stable premixed combustion had been validated by laboratory experiments. Lean blow-off, stability, and NO_x and CO emissions, were determined in terms of ϕ, and simulated $0 < FGR < 0.3$ and $0 < PRNG < 0.3$ using a $\boldsymbol{R_b} = 2.6$ cm LSB in a 18 kW water heater. The results show that PRNG improves flame stability at $\phi = 0.7$ and FGR > 0.2. PRNG was found to have no effect on NO_x but CO was reduced significantly at $\phi = 0.8$. A 1D flame model to simulate the LSB was satisfactory for predicting prompt NO_x at lean and highly dilute conditions. The results suggest that the emissions and system efficiency of a LSB boiler with PRNG can be optimized by operating at high FGR and ϕ closer to stoichiometry. The concept may be useful in lowering emissions of other lean premixed burner designs.

Conversion efficiencies of a laboratory steam reformer using two catalysts were determined to estimate the reactor volume and steam requirements for industrial boilers. An advanced Sud Chemie catalyst demonstrated higher conversion efficiency at lower temperatures (500 - 650 C) with little drop in conversion efficiency at high space velocities. These results indicate that the reformer can be small and can follow load change without changing the reformer feed rate.

Acknowledgements

References

[1]   Keller, J.O., Bramlette, T.T., Barr, P.K., and Alvarez, J.R., *Combust. Flame* 99:460 (1994).

[2]   Bradley, D., Gaskell, P.H., Gu, X.J., Lawes, M., and Scott, M.J., *Combustion and Flame* 115:515 (1998).

[3]   Brewster, B.S., Cannon, S.M., Farmer, J.R., and Meng, F.L., *Progress in Energy and Combustion Science* 25:353 (1999).

[4]   Baukal, C.E. and Schwartz, R.E., "The John Zink Combustion Handbook," Tulsa, OK: John Zink Co., LLC, 2001, pp. 750.

[5]   Cheng, R.K., Yegian, D. T., Miyasato, M. M., Samuelsen, G. S., Benson, C. E., Pellizzari, R., and Loftus, P., *Trans Comb. Inst.* 28 (2000).

[6]   Yegian, D.T., Cheng, R.K., *Combust. Sci. Technol.* 139:207 (1998).

[7]   Ren, J.-K., Qin, W., Egolfopoulos, F.N., Mak, H., and Tsotsis, T.T., *Chemical Engineering Science* 56:1541 (2001).

[8]   Chan, C.K., Lau, K.S., Chin, W.K., and Cheng, R.K., *Proc. Comb. Inst.* 24:519 (1992).

[9] Cheng, R.K., *Combust. Flame* 101:1 (1995).

[10] Bedat, B. and Cheng, R.K., *Combust. Flame* 100:485 (1995).

[11] Cheng, R.K. and Yegian, D.T., "Mechanical Swirler for a Low-NOx Weak-Swirl Burner," US Patent # 5879148 (1999).

[12] Syred, N. and Beer, J.M., *Combust. Flame* 23:143 (1974).

[13] Beer, J.M. and Chigier, N.A., *Combustion Aerodynamics*, Applied Science Publishers Ltd., London, 1972, p. 100.

[14] Lilley, D.G., *AIAA Journal* 15:1063 (1977).

[15] Cheng, R.K., Schmidt, D.A., Arrelano, L., and Smith, K.O., *2001 International Joint Power Generation Conference*, Paper IJPGC-01 19005 (2001). http://eetd.lbl.gov/aet/combustion/reprints/

[16] Yegian, D.T. and Cheng, R.K., *American Flame Research Committee International Symposium*, 1996.

[17] Plessing, T., Kortschik, C., Peters, N., Mansour, M.S., and Cheng, R.K., *Proc. Comb. Inst.* 28:359 (2000).

[18] Kee, R.J., Grcar, J.F., Smooke, M.D., and Miller, J.A., *A Fortran program for modeling steady laminar one-dimensional premixed flames*, 1985, SAN85-8240.

[19] Smith, G.P. et. al., *http://www.me.berkeley.edu/gri mech/*,

[20] Kee, J.K., Rupley, F.M., Meek, E., and Miller, J.A., *Chemkin: A fortran chemical kinetics package for the analysis of gas-phase chemical and plasma kinetics*, 1996, SAN96-8216.

[21] Bowman, C.T., "Chemistry of Gaseous Pollutant Formation and Destruction," in *Fossil Fuel Combustion - A Source Book*, W. B. A. F. Sarofim, Ed.: John Wiley Sons, Inc., 1991, pp. 866.
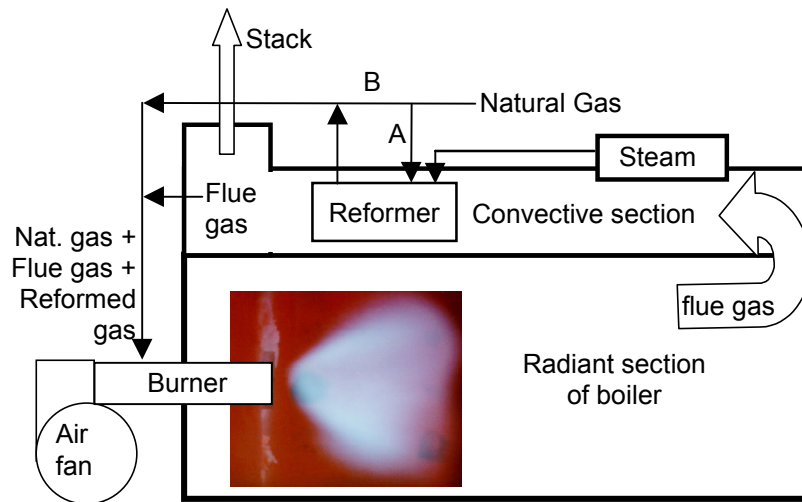
Figure 1. Adaptation of FGR/PRNG concept to packaged boiler of 300 KW to 8 MW. Picture shows a 0.6 kW flame generated by a R_b = 3.8 cm LSB.
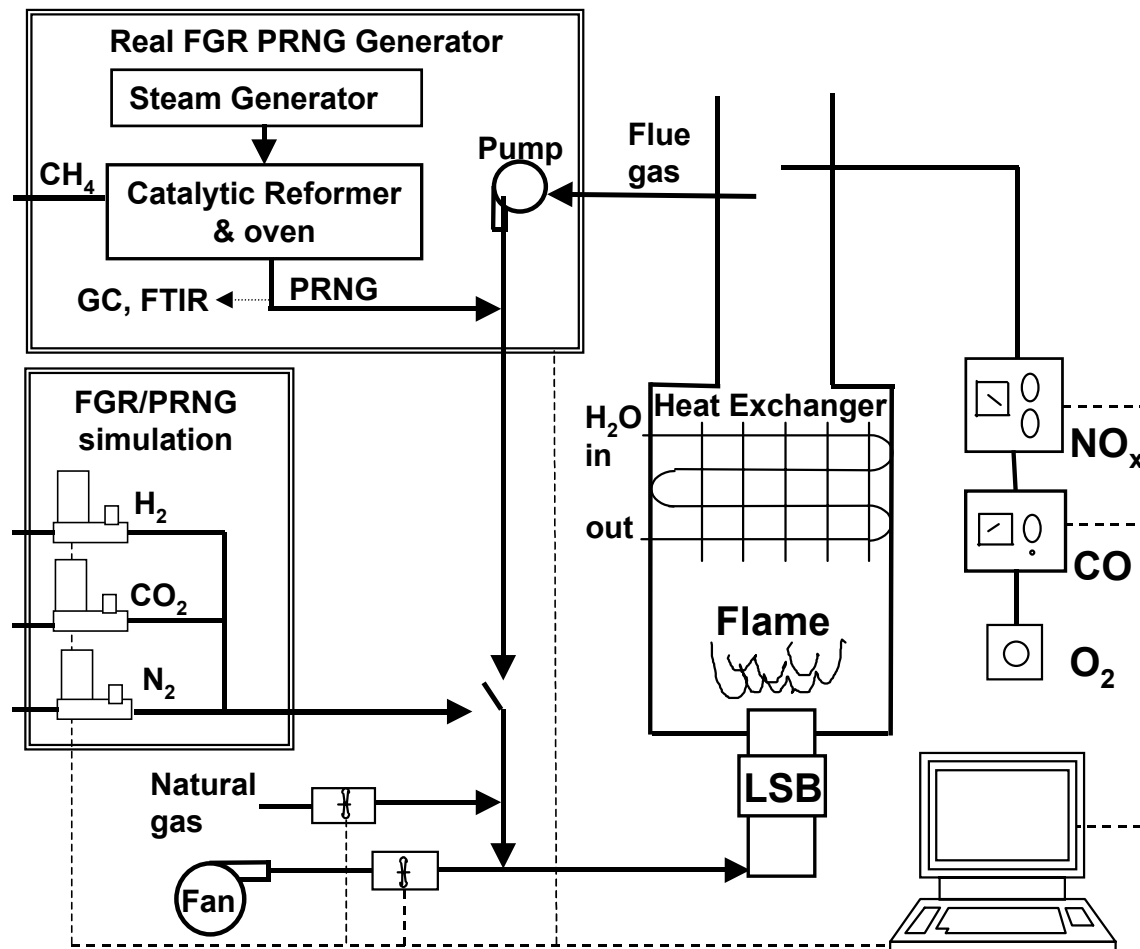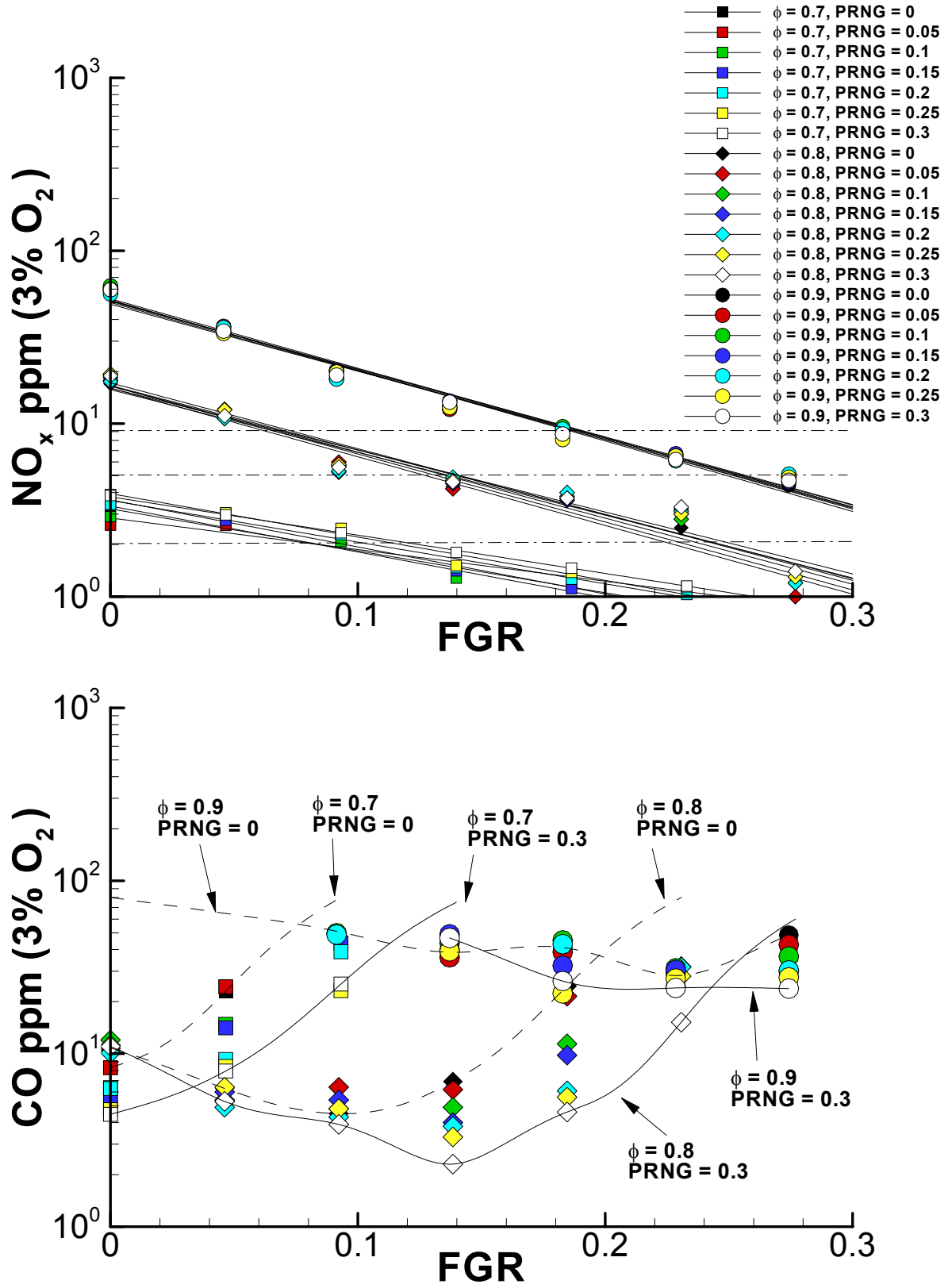

Figure 2. Schematics of laboratory setup.

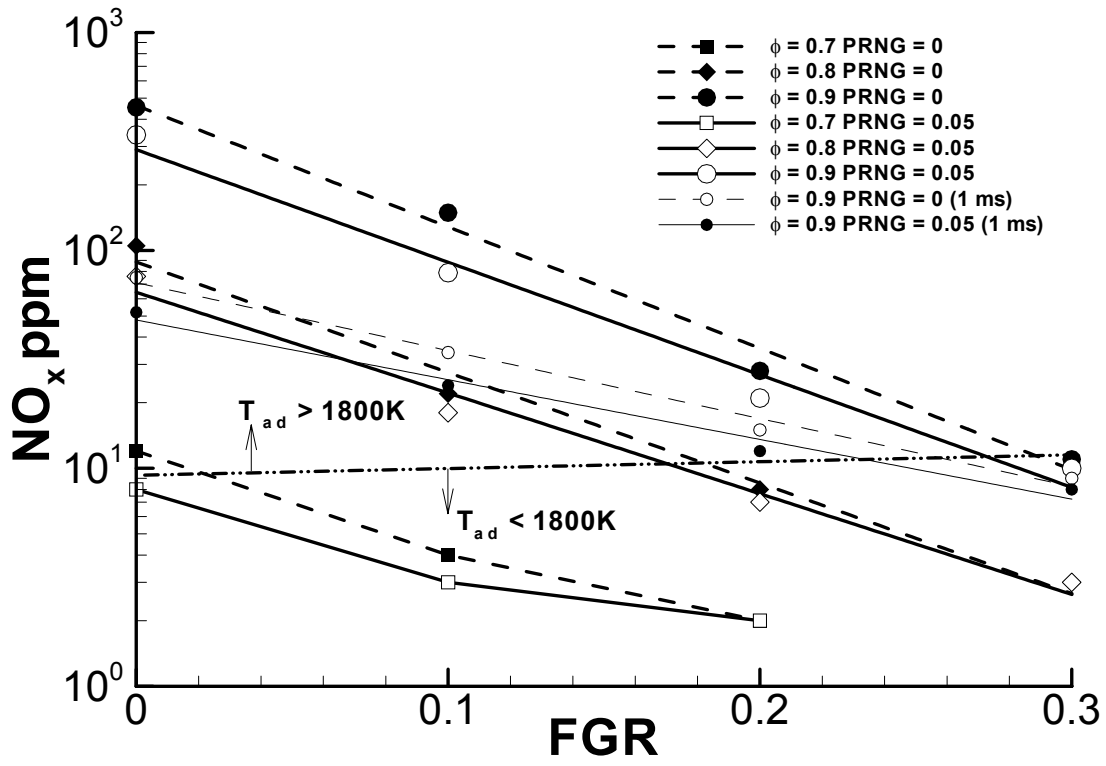Figure 3. NO$_x$ and CO emissions as functions of ϕ and simulated FGR and PRNG.

Figure 4.   1D calculation of NO$_x$ emissions as a function of ϕ, FGR and PRNG = 0 and 0.05. The dotted dashed line is the 1800 K adiabatic flame temperature contour.
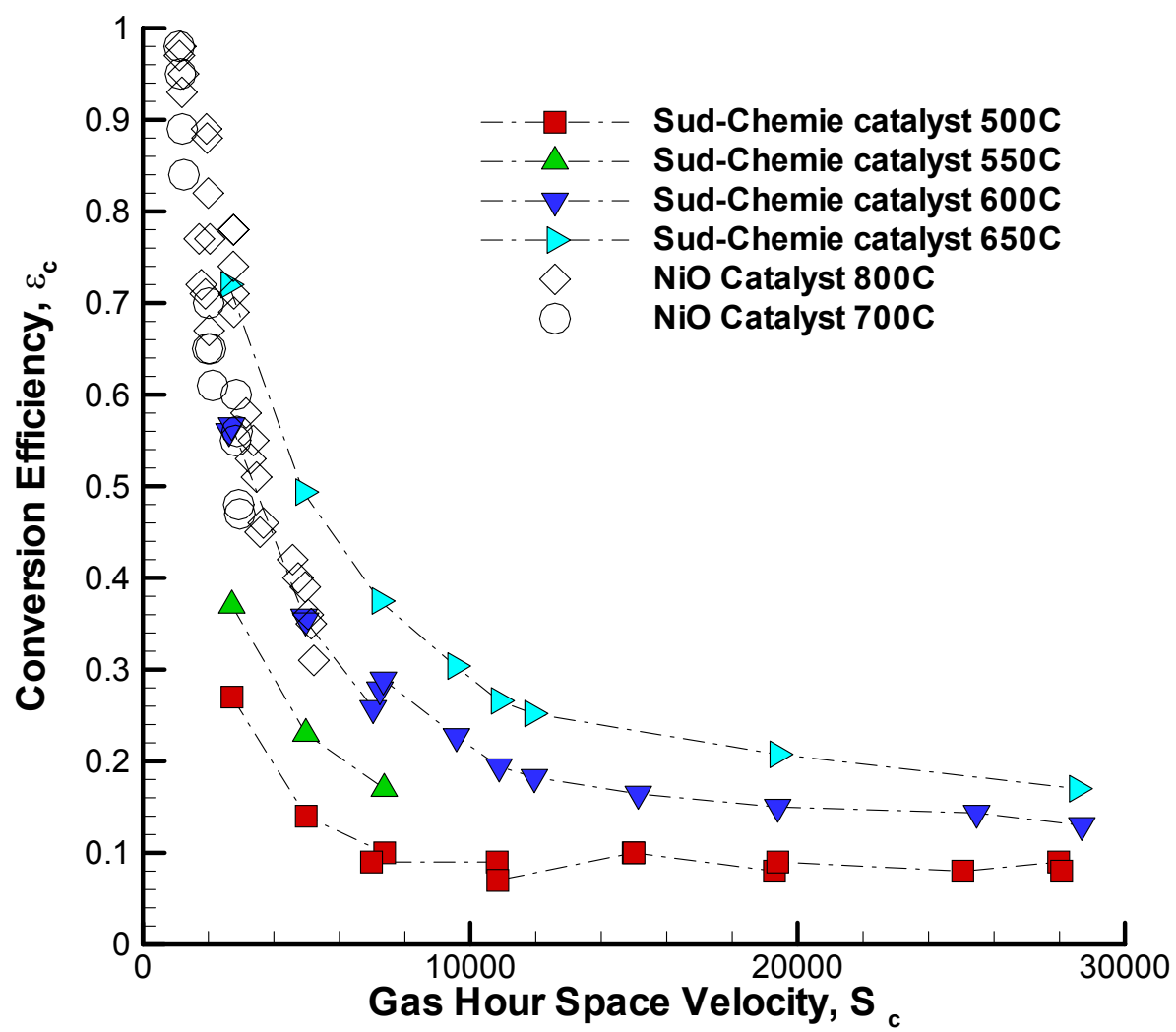
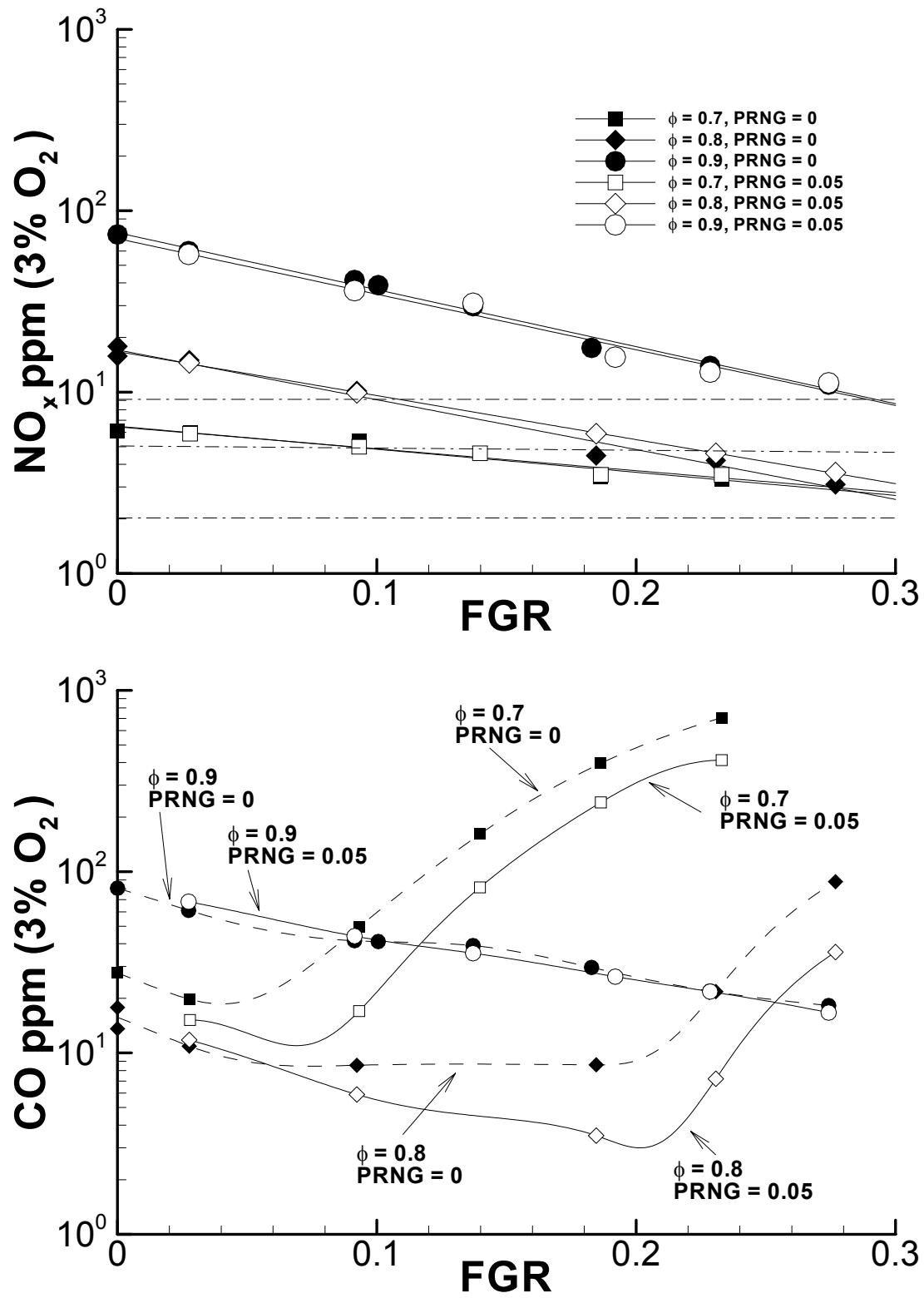Figure 5. Comparison of the partial reforming conversion efficiencies of two catalysts.

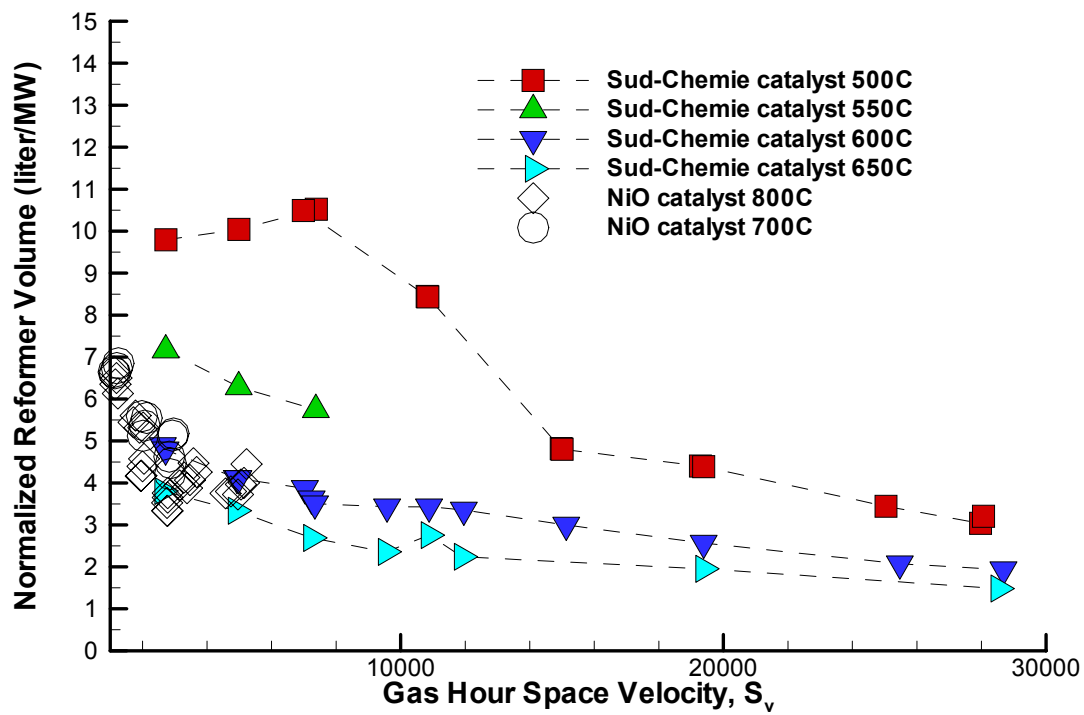Figure 6. NO_x and CO emissions as functions of ϕ, external FGR and PRNG from a catalytic reformer.

Figure 7. Normalized reformer volume per MW for boilers requiring 0.1 PRNG.